

**VERIFICATION OF NON-ISOLATED LCC RESONANT
FULL BRIDGE DC-DC CONVERTER
FOR SOLAR PHOTOVOLTAIC SYSTEMS**

By

TEOH VOON MIN

**A Dissertation submitted for partial fulfilment of the requirement for
the degree of Master of Science
(Electronic Systems Design Engineering)**

August 2015

ABSTRACT

Awareness about global warming and fastly depleting fossil fuels has intensified researcher's interest toward exploration of renewable energy resources. Among these renewable resources, photovoltaic (solar energy) is getting more attention because of its potential to be the greatest contributor of electrical energy generation. Generally DC-DC converters are used to interface solar panels with inverter which converts dc power to ac. The function of dc-dc converter is basically to step up the low dc voltage to desired higher output voltage level. Conventional switch mode dc-dc converters have problems of high switching loss and EMI. Resonant converters on the other hand have low switching loss and EMI when they operate under ZVS conditions. The aim of this research work is to explore the feasibility of a non-isolated series-parallel resonant dc-dc converter for application in PV systems. Accordingly, the working action, analysis and design procedure of series-parallel resonant full-bridge dc-dc converter is described in detail. To evaluate the performance of converter both simulation and experimental studies are carried out. First of all, converter is simulated using LT-Spice to evaluate the capability of converter to step-up dc voltage from 30V to 300V. It is shown that converter can provide desired voltage gain both for nominal and light loads with theoretical maximum efficiency up to 94%. Finally a low power laboratory prototype of the converter is built to test and evaluate the performance of the converter. The experimental results show promising performance of the converter up to 88% efficiency at 75 kHz resonance frequency. Therefore, this converter is suitable for application in PV systems where galvanic isolation is not necessary.

ABSTRAK

Kesedaran mengenai kesan rumah hijau dan semakin berkurangan bahan api fosil telah meningkatkan minat penyelidik ke arah penerokaan sumber tenaga boleh diperbaharui. Antara sumber-sumber yang boleh diperbaharui, tenaga solar semakin perhatian yang lebih kerana ia berpotensi untuk menjadi penyumbang terbesar penjanaan tenaga elektrik. Secara umumnya, penukar dc-dc digunakan untuk pemproses panel solar dengan penyongsang yang menukar kuasa elektrik dari dc-ac. Fungsi penukar dc-dc pada dasarnya untuk meningkatkan dc voltan ke tahap lebih tinggi. Cara konvensional yang menggunakan mod suis penukar mengalami masalah kehilangan tenaga elektrik akibat pensuisan yang tinggi dan masalah gangguan EMI. Penukar salunan adalah di antara cara penukaran yang mempunyai kehilangan tenaga elektrik yang rendah akibat pensuisan dan kurang masalah EMI apabila beroperasi di bawah keadaan ZVS. Tujuan penyelidikan ini adalah untuk meneroka kemungkinan yang salunan dc-dc penukar bukan terpicil siri-selari untuk aplikasi dalam sistem PV. Tindakan, analisis dan reka bentuk prosedur kerja siri-selari salunan sepenuh jambatan dc-dc penukar diterangkan secara terperinci. Untuk penilaian prestasi reka bentuk penukar, simulasi dan kajian eksperimen dijalankan keduanya. Simulasi litar penukar menggunakan LT-Spice untuk menilai keupayaan penukar untuk meningkatkan voltan dc dari 30V ke 300V dengan efisiensi setinggi 94%. Penilaian telah menunjukkan penukar yang boleh memberikan gandaan voltan diinginkan untuk beban nominal dan beban ringan. Akhirnya prototaip makmal kuasa yang rendah siap dibina untuk menguji dan menilai prestasi penukar. Keputusan eksperimen menunjukkan prestasi baik dengan prototaip mencapai efisiensi setinggi 88%. Oleh itu, penukar ini sesuai untuk aplikasi dalam sistem PV di mana pengasingan galvanik tidak diperlukan.

ACKNOWLEDGEMENT

First and foremost, I would like to thank my devoted parents and parents-in-law for their unconditional support all the time while both my wife and myself pursuing our dream in fulfilling master degree in USM. Also, I wish to give my utmost appreciation, gratitude and love to my wife, Chua Cheah Chin, my loving daughters, Zhi Qi and Zhi Lin for being my private source of endless joy, happiness and encouragement round the clock.

My personal recognition for the most important pillar behind this project is my supervisor, Dr Shahid Iqbal. My greatest gratitude to Dr Shahid for giving me the opportunity to explore my academic interest and practical implementation with this work. I would not be able to complete the project within the time given without Dr Shahid advice and guidance throughout the whole semester. I would also like to express heartfelt thanks for my friends in USM and my colleagues in Intel Malaysia for engaging technical discussion and provided their invaluable opinions. Not forgetting USM laboratory technical staff who provided seamless cooperation during the prototype experiments were carried out and supported my hardware component requests.

I definitely treasure the journey of learning, discovering, maturing and building bonds with friends and family. All will remain as memories which can last a lifetime.

CONTENTS

ABSTRACT	i
ABSTRAK.....	ii
ACKNOWLEDGEMENT.....	iii
CONTENTS	i
LIST OF FIGURES.....	iv
LIST OF TABLES	vii
ACRONYMS.....	viii
CHAPTER 1	1
1.1 General background	1
1.2 Problem Statement	6
1.3 Objectives.....	6
1.4 Organization of the Thesis	6
CHAPTER 2	8
2.1 Introduction	8
2.2 Step up DC-DC Converter Review.....	8
2.2.1 DC-DC Boost Converter Operation	9
2.2.2 Limitation of Conventional Boost converter.....	11
2.3 Switch Mode and Resonant Mode Review	11

2.4	Review of Resonant Converter Topologies.....	16
2.4.1	Series resonant converter	16
2.4.2	Parallel resonant converter	18
2.4.3	Series-parallel resonant converter.....	19
2.5	Resonant converter operation mode	20
CHAPTER 3		24
3.1	Introduction	24
3.2	The Proposed Non Isolated DC-DC Converter	24
3.3	Analysis of Steady State Operation	25
3.3.1	Mode 1 ($t < t_0$).....	27
3.3.2	Mode 2 ($t_0 < t < t_1$)	28
3.3.3	Mode 3 ($t_1 < t < t_2$)	29
3.3.4	Mode 4 ($t_2 < t < t_3$)	30
3.3.5	Mode 5 ($t_3 < t < t_4$)	31
3.3.6	Mode 6 ($t_4 < t < t_5$)	32
3.3.7	Mode 7 ($t_5 < t < t_6$)	33
3.4	DC Gain analysis of Series-Parallel Resonant Converter	34
CHAPTER 4		39
4.1	Introduction	39
4.2	Design Procedure for the Proposed Converter	39
4.2.1	Design Specifications.....	40

4.2.2	Determination of the Size of Circuit Components.....	40
4.2.3	Verification of Design using LT-Spice Simulation	42
4.3	Design of Scaled Down Experimental Prototype	46
4.3.1	Design Specifications.....	46
4.3.2	Determination of the Size of Circuit Components.....	46
4.3.3	Selection of Circuit Components.....	49
4.4	Implementation of Experimental Prototype	51
CHAPTER 5		54
5.1	Introduction	54
5.2	Results and Discussion.....	54
5.3	DC Gain and Efficiency Analysis.....	62
CHAPTER 6		65
REFERENCES		67
APPENDIX		70

APPENDIX

Appendix I	Pin definition of UCC25600 resonant microcontroller by Texas Instruments	70
Appendix II	UCC25600 resonant microcontroller block diagram	71
Appendix III	Optocoupler HCPL-3140 datasheet by Avago Technologies.....	72
Appendix IV	Schottky diode MBR10150 datasheet.....	73
Appendix V	Schottky diode MBR10150 maximum current rating.....	74

LIST OF FIGURES

Figure 1.1: Global renewable electricity production by region.....	1
Figure 1.2: Simplified PV system of two PV panels with boost DC-DC converters and a central DC-AC inverter	3
Figure 1.3: Overview of micro inverters challenges at present day	4
Figure 1.4: Comparison of key characteristics of major Solar PV system topologies for commercial or residential application.	5
Figure 1.5: Commercial micro inverters commonly advertised features	5
Figure 2.1: Hierarchical View of Step Up DC-DC Converter	9
Figure 2.2: Single switch boost converter.....	9
Figure 2.3: Switch control and current waveforms of basic boost converter.....	10
Figure 2.4: Block diagram of switch mode PWM DC-DC Converter.....	12
Figure 2.5: Hard switching current and voltage waveform.....	12
Figure 2.6: Block diagram of DC-DC resonant converter	13
Figure 2.7: Transient noise comparison for PWM and resonant converters.....	14
Figure 2.8: Bandwidth comparison among PWM, Quasi-resonant converter (QRC) and resonant converter (RC)	15
Figure 2.9: Example of series resonant converter.....	16
Figure 2.10: SRC converter gain curve for above resonance	17
Figure 2.11: Example of parallel resonant converter.....	18
Figure 2.12: SRC converter gain curve for above resonance	19
Figure 2.13: Example of series-parallel resonant converter.....	20
Figure 2.14: Soft switching voltage and current waveform	21
Figure 2.15: Example of voltage and current operating at above resonance.....	22
Figure 2.16: Possible spikes on waveform due to hard switching.....	23

Figure 3.1: The proposed non-isolated LCC resonant converter.....	25
Figure 3.2: Waveforms at steady state	26
Figure 3.3: Mode 1 operation during $t < t_0$	27
Figure 3.4: Waveforms of Mode 1 are represented by shaded area.....	27
Figure 3.5: Mode 2 operation during $t_0 < t < t_1$	28
Figure 3.6: Mode 2 (dead time) represented in shaded area.....	28
Figure 3.7: Mode 3 operation during $t_1 < t < t_2$	29
Figure 3.8: Mode 3 represented in the shaded area	29
Figure 3.9: Mode 4 operation at $t_2 < t < t_3$	30
Figure 3.10: Mode 4 represented in the shaded area.....	30
Figure 3.11: Mode 5 operation at $t_3 < t < t_4$	31
Figure 3.12: Mode 5 represented in the shaded area.....	31
Figure 3.13: Mode 6 operation during $t_4 < t < t_5$	32
Figure 3.14: Mode 6 represented in the shaded area.....	32
Figure 3.15: Mode 7 operation during $t_5 < t < t_6$	33
Figure 3.16: Mode 7 represented in the shaded area.....	33
Figure 3.17: Square wave input voltage and fundamental component	34
Figure 3.18: Equivalent ac resistor of rectifier seen by resonant circuit.....	35
Figure 3.19: AC equivalent representations for LCC resonant converter.....	35
Figure 3.20: Q Curves of the proposed series parallel resonant frequency ($C_s = 2C_p$)	37
Figure 3.21: Q Curves of the proposed series parallel resonant frequency ($C_s = C_p$)	38
Figure 4.1: Proposed converter constructed in LT-Spice environment	43
Figure 4.2: Simulated waveforms of designed series-parallel resonant dc-dc converter for output load power of 425W	44

Figure 4.3: Simulated waveforms of designed series-parallel resonant dc-dc converter for output load power of 210 W.	45
Figure 4.4: Schematic circuit diagram of the proposed converter.	52
Figure 4.5: Photograph of the Eagle layout of the proposed converter	53
Figure 4.6: Photograph of the experimental prototype	53
Figure 5.1: Filtered Output voltage measurement at $F_s = 75$ kHz (a) simulation, (b) measurement.....	55
Figure 5.2: Filtered Output voltage measurement at $F_s = 80$ kHz (a) simulation, (b) measurement.....	57
Figure 5.3: Filtered Output voltage measurement at $F_s = 85$ kHz (a) simulation, (b) measurement.....	58
Figure 5.4: Filtered Output voltage measurement at $F_s = 120$ kHz (a) simulated, (b) measurement.....	60
Figure 5.5: Filtered Output voltage measurement at $F_s = 125$ kHz (a) simulated, (b) measurement.....	61
Figure 5.6: Gain conversion comparison graph.....	63
Figure 5.7: Efficiency comparison graph.....	64

LIST OF TABLES

Table 4.1 Input specifications of the step up converter.....	40
Table 4.2 Input specifications of the step up converter (prototype)	46
Table 5.2: Summary of gain conversion.	63

ACRONYMS

AC	Alternating Current
CEC	California Energy Commission
DC	Direct Current
EMI	Electromagnetic Interference
ESL	Equivalent Series Inductance
ESR	Equivalent Series Resistance
MPPT	Maximum Power Point Tracking
MTRMR	Medium Term Market Report
PRC	Parallel Resonant Converter
PV	Photovoltaic
PWM	Pulse Width Modulation
SI	Signal Integrity
SMPS	Switch Mode Power Supply
SRC	Series Resonant Converter
TWh	Terawatt hours
ZCS	Zero Current Switching
ZVS	Zero Voltage Switching

CHAPTER 1

INTRODUCTION

1.1 General background

Renewable energy demand and production has been growing steadily across the globe to ease fossil fuel import bills. United States and European Union have specifically set baseline target to reduce its greenhouse gas emissions by 20%, increase the share of renewable energy to at least 20% of consumption. According to International Energy Agency last year report [1], from the previous year 2013, global renewable electricity generation rose to an estimate of 240 terawatt hours (TWh) to reach nearly 5070 TWh and accounted for almost 22% of total power generation as shown in Figure 1.1. The renewable capacity expansion was faster than that foreseen in MTRMR 2013, with deployment of hydropower and solar PV exceeding expected forecast.

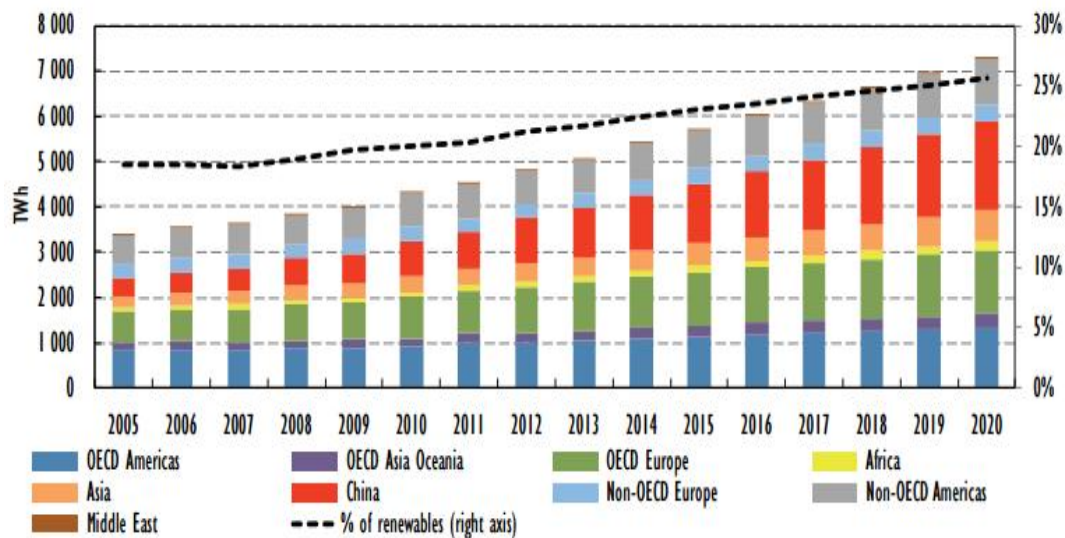


Figure 1.1: Global renewable electricity production by region

Solar photovoltaic systems are becoming one of the most appealing green energy preference to industrial and household, which can be seen deployed for tall-building-integrated systems, residential rooftop system or dedicated solar farms. Several type of inverter system architectures exist in the solar PV systems. One of the most common approaches involves a single grid-tie inverter connected to a daisy-chain string of PV panels. Even though this approach is fairly easy for actual deployment, there are at least two limitations to this approach. Firstly, the maximum power point tracking (MPPT) is performed for the entire series string of panels, which is not optimal given variations among panels and variations in illumination of each panel [2-3]. Secondly, a permanent defect or even a temporary shade to a single panel in an array, which is controlled by a single inverter, limits the performance of the entire string [2-3]. Alternative approach in managing solar panels is through the use of micro inverters which are power converters rated at a few hundred of watts each, directly integrated with individual panel before going to the household supply or AC grid [4]. This way each solar panel energy harvesting can be more efficient individually as compared to the series-connected string of modules. Micro inverters benefit from their modularity, capable of plug-and-play installation by users with limited knowledge of electrical systems.

Looking further into photovoltaic (PV) systems usually comprise of one or more parallel strings with series connected PV panels. Due to the series connection, it is inherently implies that the output currents of all PV panels are the same. However if the PV panels in the string receive unequal irradiances, the condition of equal current generation within that string will no longer be fulfilled. Hence the total power which can be harvested from the string decreases below the theoretical possible available power. This is due to the fact that the shaded PV panels are being bypassed if the string current is kept at above its level to match the unshaded panels [5]. Or in another way, the DC-AC inverter

can reduce the current level to average between shaded and unshaded panel. In either way, it will be a compromise to sub-optimal operation the PV systems as a whole. As a solution, each PV panel equipped with a DC-DC boost converter and its output is connected in parallel for central DC-AC inverter input as illustrated in Figure 1.2. So an appropriate converter topology with a high step-up ratio and high conversion efficiency is critical, boost converter will be reviewed in Chapter 2.

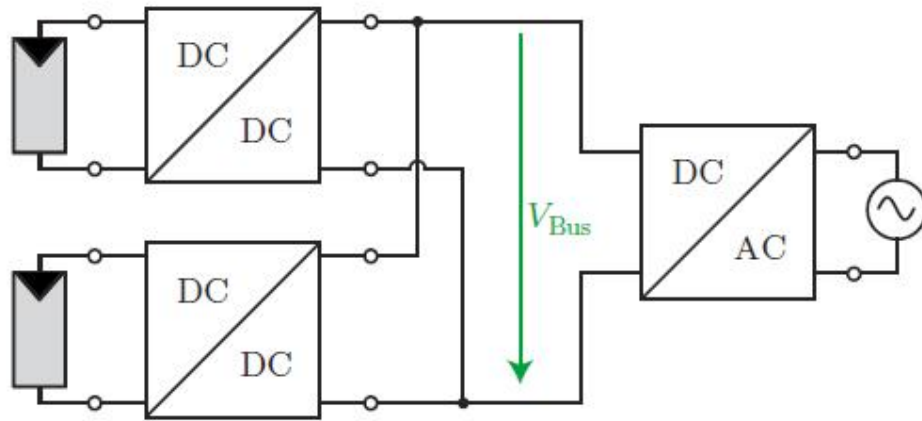


Figure 1.2: Simplified PV system of two PV panels with boost DC-DC converters and a central DC-AC inverter

Micro inverters embrace a modular system configuration and allow for the concept of inverter-per-panel design. Decentralized inverter scheme eliminates the need for a single point of operation and failure in a PV system. The hardware components and software by which the system adjusts voltage to find the PV system's maximum power point is known as the maximum power point tracker (MPPT). While traditional PV system topologies limit maximum power point tracking to the inverter level, micro_inverters and embedded power optimizer topologies relocate the MPPT to the level of the module [6]. Any issue relating to how MPPT will be applied to the entire PV system is no longer a concern as each micro inverter-panel pair is itself a system [7].

When considering the application of micro inverters, it is always important to first consider logistics. The primary benefits of micro inverters are the cost of installation, the

ease of power output scalability and resistance to shading. However, these benefits are made less valuable in large scale operations such as solar PV farms. On these scales, the cost thresholds to installation are negligible, the cost per watt of central inverters scales much more favorably and panels are clear of shade and cleaned regularly [9]. Unlike a residential rooftop that is multi-angled and difficult to work with, solar farmland is chosen to suit energy production and not retro-fitted vice versa. As such, a practical place for micro inverters to outperform central inverters is in a residential or small commercial installation. When facing challenges such as multi-angled roofing and big sum of installation cost for central inverter systems, micro inverters can become very feasible options [8]. Based on the simulation study by O'Callaghan, Lynette [9], Building Integrated PV (BIPV) systems are approximately 20 to 25%, due to shade, mismatch, differences in orientation and inclination, and temperature effects. 59.4% of the simulations showed gains in AC power by using the parallel modular converter system, with a maximum gain of 10.74%, when compared with the series configuration. Some of the challenges faced by micro-inverters design are as shown in Figure 1.3.

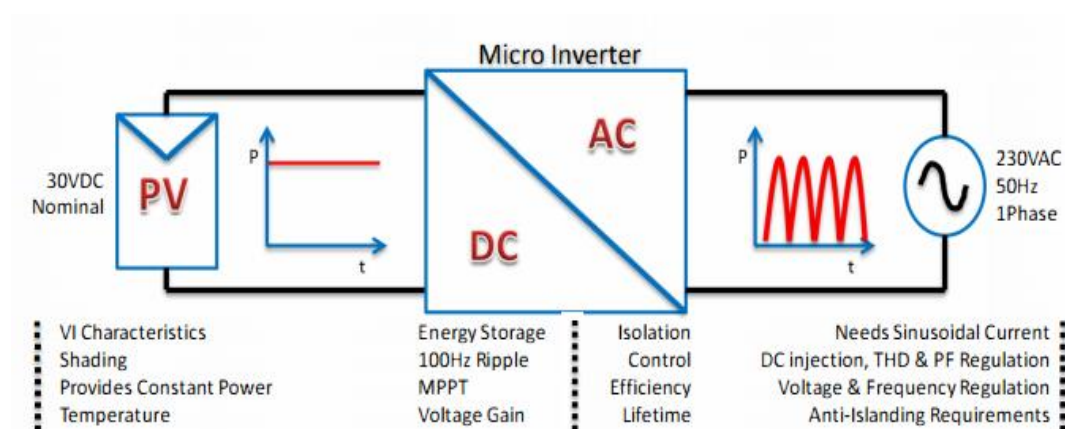


Figure 1.3: Overview of micro inverters challenges at present day

Ref. [7] reviews the current state of the micro inverter, design issues relating to grid tied DC/AC power conversion and future directions for the cloud operation of micro inverters in residential micro grids. Worthy summary of comparisons among existing solar inverters including residential type are shown in Figure 1.4 and Figure 1.5. This is one of the primary motivation for this research title on DC-DC resonant converter which can be largely applicable for residential micro inverters.

Characteristic	Unit	Traditional Central Inverter	Traditional Central Inverter with Smart PV Optimisers	Micro Inverter or AC Module
Typical Upfront Cost per Watt of Inverter	\$USD	\$0.40*	<\$0.52	\$0.52*
Installation Cost/Difficulty	Low/High	High	High	Low
Mass Producability	Low/Med/High	Low	Med	High
Typical Installation Power Range	Watts	>1.5kW	>1.5kW	>200W
Size Scalability of Installation	Low/High	Low	Low	High
Maximum CEC** Inverter Efficiencies	%	95%-97%***	95%-97%***	95%-96%****
MPPT for each PV panel	Low/High	No	Yes	Yes
Entire System Reliability	Low/Med/High	Med	Med	High
Temperature Issues for Inverter	Low/High	Low	Low	High
High Voltage DC Safety Issues	Yes/No	Yes	Yes	No

Figure 1.4: Comparison of key characteristics of major Solar PV system topologies for commercial or residential application.

Note: *[10], **The "California Energy Commission" (CEC) weighted efficiency (focusing mostly on the 50% & 75% power levels), ***[11], **** (see Figure 4).

Micro Inverter	Enecsys 300-60-MP	Enphase M215	GreenRay SunSine AC Module	Sunwave AC Module	Solar Bridge Pantheon 2	SMA SunnyBoy 240-US	Power One Micro-0.25-1
AC Power	300W	215W	200W	~220W	238W	240W	250W
MPPT Range	24V-35V	22V-36V	-	-	18-37V	23V-32V	25V-60V
PF	>0.95	>0.95	>0.98	>0.98	>0.99	-	>0.95
THD	<5%	-	<5%	<5%	<5%	-	-
Efficiency*	96% CEC	96% CEC	-	91.5% CEC Min.	93.2% Euro	95% CEC	95.4% Euro
Weight	1.65kg	1.6kg	Integrated	Integrated	1.6kg	1.3kg	1.65kg
Ambient Max	-40°C to 85°C	-40°C to 65°C	-20°C to 45°C	-40°C to 85°C	-40°C to 65°C	-40°C to 65°C	-40°C to 65°C
Warranty	25 Years	-	20 Years	-	25 Years	-	-

Figure 1.5: Commercial micro inverters commonly advertised features

1.2 Problem Statement

Resonant converters designed for step-up applications normally employ transformer to produce desired step-up ratio. In such converters, conversion ratio can be easily controlled by ensuring the transformer primary to secondary winding turn's ratio. However, transformer can be bulky and costly. Unlike commercial solar PV systems, residential applications may not necessarily requires isolation for most cases. The challenge is to address the high conversion ratio with a non-isolated DC-DC resonant converter and achieve low cost at the same time.

1.3 Objectives

The main objectives of this work are

1. To propose a non-isolated series-parallel resonant dc-dc converter for PV application.
2. To study the feasibility of non-isolated series-parallel resonant converter for PV systems up to 450W range.
3. To verify the operation, performance and advantage of proposed converter with low power prototype.

1.4 Organization of the Thesis

This thesis consists of six chapters.

Chapter 1 is the introduction. It briefly introduces the design challenges for low voltage, high current DC-DC converter and power distributed architectures in photovoltaic application where DC-DC converter may be used. Brief comparison between traditional PWM converter and resonant converter is also given. Chapter 1 provides motivation and level sets objectives for the research contributions presented in this thesis.

In Chapter 2, literature review of the topics is presented. First of review of conventional switched mode dc-dc converter is presented. The advantages and disadvantages of switch mode dc-dc converters are given. Finally a detailed review of resonant converters is presented. From the review it is found that series-parallel resonant dc-dc converter has the potential to provide high step-up voltage gain. Consequently, a series-parallel resonant dc-dc converter has been selected to be explored further for its application in PV systems.

Chapter 3 is the methodology. In this chapter the structure of circuit, its operation and analysis is described. DC gain transfer function of the converter is derived and plot for various values of capacitor ratios and quality factory is given.

In Chapter 4, the design and implementation procedure of proposed converter is described. The step by step procedure for the selection of circuit components is given. The equations which were developed in chapter 3 are used to determine the size of circuit components. Based on the values of LC components, the resonant frequency of the converter was calculated. Then a UCC25600 resonant mode controller was designed to operate the converter above resonance for realizing ZVS operation. The bootstrap technique was utilized to power up the upper isolated gate drive circuits.

Chapter 5 presents the simulation and experimental results from the simulation and laboratory prototype of the converter respectively. A number of simulation and experimental waveform taken at different frequencies are presented in this chapter to show the regulation capability of the converter. All the simulation and experimental results are discussed and compared.

Finally, Chapter 6 concludes the overall thesis. Future works that can be implemented are discussed in this chapter.

CHAPTER 2

LITERATURE REVIEW

2.1 Introduction

This chapter provides literature review on step up dc-dc converters and briefly discussed about the current state of art for high step-up dc-dc converters in section 2.2. Next section 2.3 provides review of conventional switched mode dc-dc converter is presented in comparison with resonant mode converters. The advantages and disadvantages of switch mode dc-dc converters are given. The area of interest for this thesis is resonant converters, three types of resonant converters will be reviewed in details in section 2.4.

2.2 Step up DC-DC Converter Review

Commonly used commercial photovoltaic panels deliver electric power at the output voltage range of $12V_{DC}$ to $70V_{DC}$ [12]. To make use of the energy sources, the PV panels output should be boosted to system V_{BUS} as shown in Figure 1.2 in order to match the electric grid standards. In order to meet stringent requirements of electric grid requirements, high efficiency and high voltage step-up dc-dc converters will be reviewed in this section. Numerous type of step-up dc-dc converters can be loosely categorized as shown in Figure 2.1. Comparison of dc-dc boost converters is presented in [13-14]. For non-resonant converters, the gain is generally controlled by the duty cycle as the voltage gain formula deals with the duty cycle primarily. However, there are limitations due to this as duty cycle being set close to one for high gain. Limitations will be explain in details in Section 2.2.2.

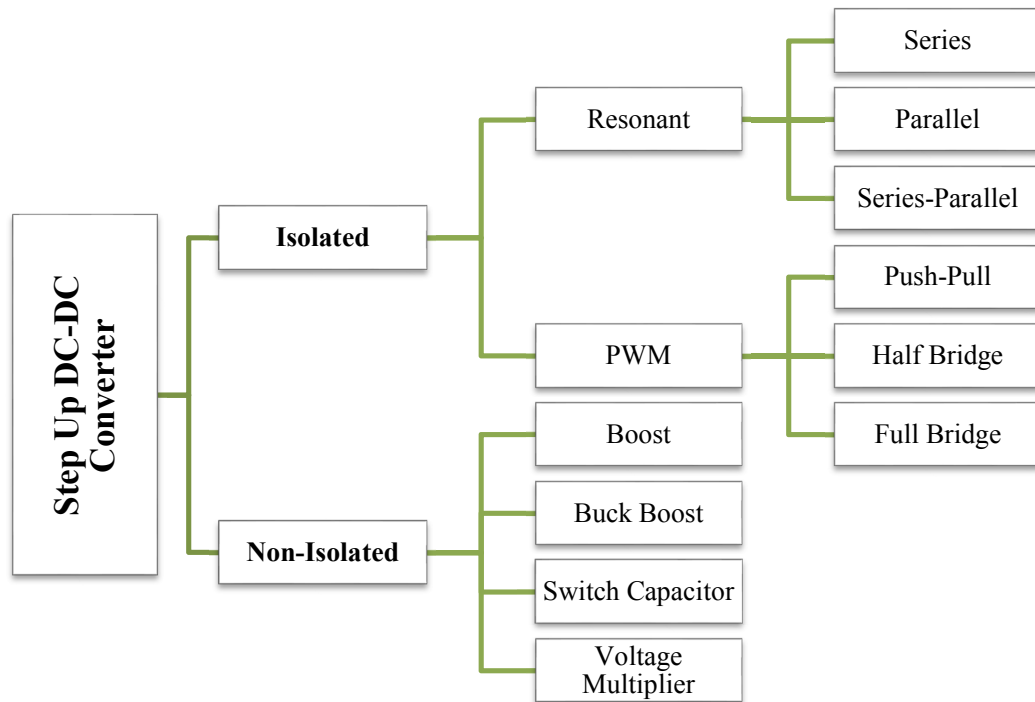


Figure 2.1: Hierarchical View of Step Up DC-DC Converter

2.2.1 DC-DC Boost Converter Operation

Boost converters are used in applications where high voltage and high power requirements for the output but the input supply is small for example PV solar panel gives 20-40Vdc. This section will review principle of operation for conventional DC-DC boost converter as shown below in Figure 2.2.

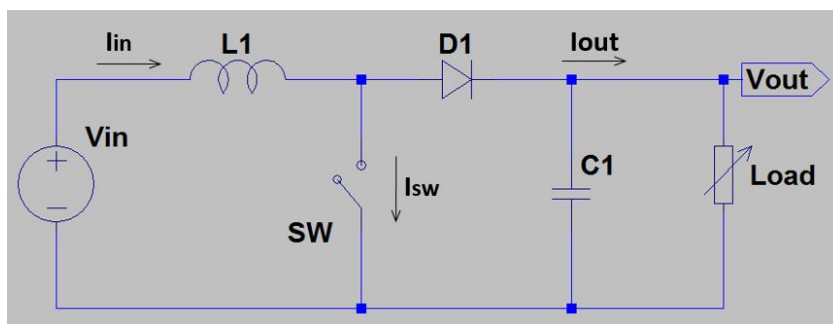


Figure 2.2: Single switch boost converter

During the start up, as MOSFET gate being driven, MOSFET switch is closed and current charge build up energy and stored in its magnetic field. During the energy storing, there is no current flowing through the other side of the circuit since the diode capacitor and load is of higher impedance path to the input. As the gate signal becomes low, the sudden drop in current forces inductor to produce back electromagnetic force in the opposite direction to the voltage across the inductor to ensure current flows continuously. With that inductor now behaves like a voltage source, V_{L1} in series with original DC input source. Diode will see higher voltage potential due to $V_{in} + V_{L1}$, hence becomes forward bias. Since MOSFET is off, there will be no current path through the MOSFET. The resulting current will flow through D1 and charges C1 to $V_{in} + V_{L1}$ (assuming diode drop is small enough) and also supplies to the load [14]. From the current waveform in Figure 2.3, notice that the input current to the boost converter is always higher than the output current. Now assuming lossless boost conversion, output power must be equal to the in power ($P_{in} = P_{out}$) [15]. With that, the output voltage will be higher than the input voltage which is the objective of boost converter operation.

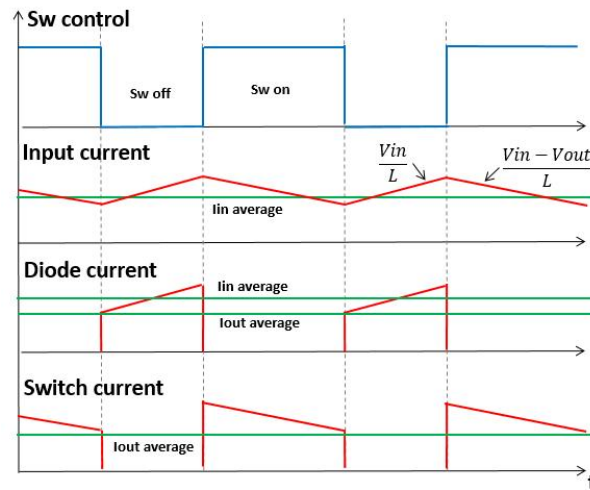


Figure 2.3: Switch control and current waveforms of basic boost converter

2.2.2 Limitation of Conventional Boost converter

Most of the conventional boost converters power gain is essentially controlled by the duty cycle. Theoretically, the gain can go up to infinite when extreme duty cycle close to one is applied. On the other side, the switch turn-off period becomes very short due to large duty cycle and forces current ripple increases significantly in high step-up conversion. Bigger size or multiple electrolytic capacitors will be required to handle the huge ripple output. Furthermore, the high switch voltage stress in order to achieve high gain is a major concern in conventional boost converter. High voltage stress directly impact the power switches and diode, as the component ratings should be higher than the output voltage. The switching loss becomes significant due to hard switching operation. For higher gain with conventional boost converter, implementation cost will increase due to filtering solution and higher voltage rating for switches and diodes.

2.3 Switch Mode and Resonant Mode Review

It has been trend of many years to reduce weight and size of power converters design which is the primary driver for continuous increase of operational switching frequencies. With higher operating frequencies, it allows size reduction of circuit magnetics and capacitors leads to more compact and cheaper cost of materials. Pulse width modulated (PWM) converters are widely known standard for present switch mode power supply (SMPS) products. The diagram of traditional SMPS with PWM converter is shown in Figure 2.4 which consists of an inverter, output rectifier and output low pass filter. Input DC voltage is chopped at switching frequency to generate square AC voltage. The rectifier output can be controlled thru duty cycle of the chopper circuit.



Figure 2.4: Block diagram of switch mode PWM DC-DC Converter

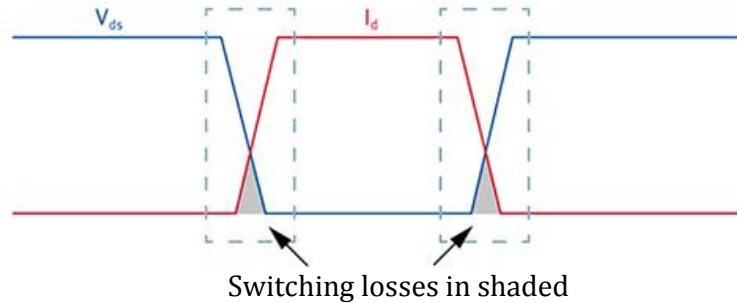


Figure 2.5: Hard switching current and voltage waveform

Hard switching occurs during the overlap of voltage and current when the MOSFET is turning on and off. Newer design of SMPS with PWM converters improves the switching loss by increasing the rate of change of voltage (dV/dt) and also the rate of change of current (dI/dt), hence the shaded area as shown in Figure 2.5 will be minimized. Nevertheless, the tradeoff of faster switching scheme is the side effect of electromagnetic interference (EMI) arises from the power regulator circuit. Power devices energy losses due to switching losses despite being controlled will still be there and it becomes relatively significant that at some point prevents further increase of switching frequency. To overcome that bottleneck, resonant frequency converters are considered as better solution since resonant circuit can help to minimize or avoid switching losses in semiconductor switches naturally. The solution is to replace the chopper switch of PWM topology with a resonant tank that effectively functions as a pseudo switch. Ideally there is no voltage across inductor and current through capacitor, so there will be very little concern for power losses.

Resonant network or usually known as the LC tank circuit has the effect of filtering higher harmonic voltages so that essentially it will respond to the fundamental harmonic and sine wave of current appears at the input to the resonant circuit as shown in Figure 2.6. As the fundamental component of the square wave input voltage (generated by the switching network) is applied to the resonant network, the resulting sine waves of current and voltage can be computed using classical AC analysis. It is important to note that the power supply load resistance is not the same load resistance which should be used in the ac analysis. The rectifier with its filter acts as an impedance transformer as far as the resonant circuit is concerned. This is due to the nonlinear nature of the rectifier [16].

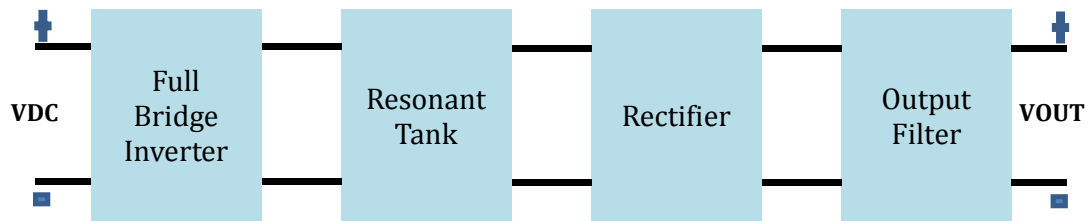


Figure 2.6: Block diagram of DC-DC resonant converter

Literature research on the aspect of noise can help to justify the motivation of proposed circuit in this thesis later. Hard switching and soft switching converters have different noise performance depending on the power, frequency range and switching techniques primarily. T. Higashi et al have examined the noise characteristics by experiment and simulation of PWM converters with schottky diode and multilayered ceramic capacitor are operating at the same input voltage of 12V, output voltage of 5V and load of 10 ohm [17]. Results from transient noise are compared in Figure 2.7.

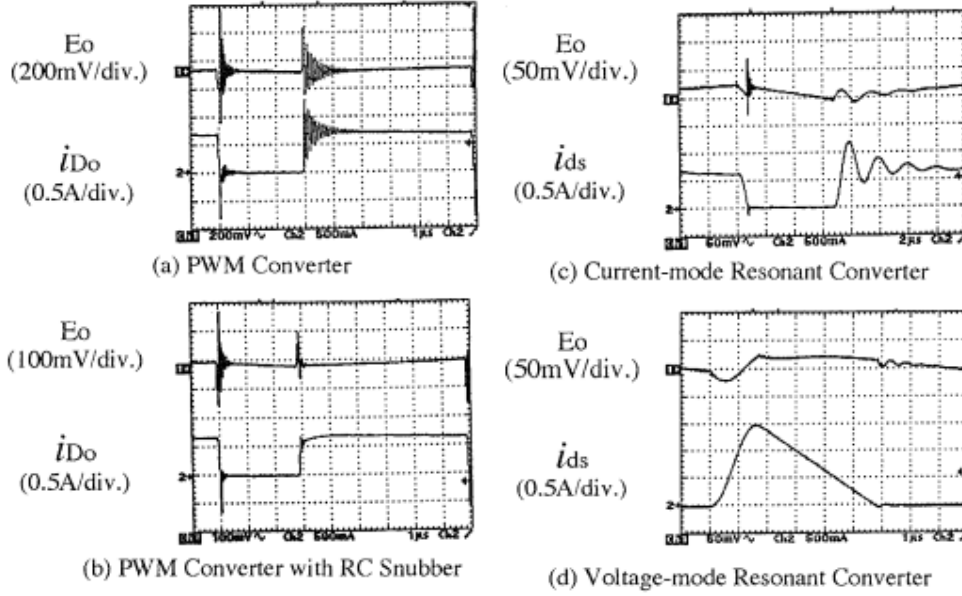


Figure 2.7: Transient noise comparison for PWM and resonant converters

Noise characteristics for PWM, PWM with snubber, Current mode resonant and voltage mode resonant converter has been quantitatively studied and compared by experiment and accurate simulation. Key discussions are summarized as follows [17]:

1. Both current mode and voltage mode resonant converters show much lower output voltage noise compared to PWM and PWM with RC-snubber type.
2. Current mode resonant converter has steep surge in output voltage compared to voltage mode counterpart.
3. Voltage mode converter shows the lowest noise performance at output stage.
4. Output surge voltage at diode's turn-off is sensitive to stored charge in diode for PWM, PWM with snubber and Current-mode resonant converters.

Due to high frequency in the design, it is common myth that resonant converters suffer more severe EMI problems than PWM converters. The main reason is that PWM converters switching frequency is fixed, so are the related harmonics. Whereas for resonant converters the switching frequency and its harmonics will be shifted accordingly along the

spectral axis as load dynamically changes. Generally, there are two kinds of electromagnetic interference (EMI) in the power supply. First, the EMI generated by the switching actions, and the control signals of active switches can be thought as the main source of this kind of EMI. Second, the EMI produced by parasitic elements, which cause turning-on and turning-off ring effects.

To minimize EMI effect, power density level in the spectrum should be as low as possible. Based on the qualitative comparison presented in, under the same modulation index β_v , quasi-resonant converter and resonant converter control signals have smaller bandwidth as compared to PWM control signal [18]. Note: modulation index β_v is the ratio of dynamic output to overall output. Y .F. Zhang, L. Yang, and C.Q. Lee presented paper which focused on control signals spectral analysis. By theoretical analysis, for the same peak variation value and same modulation frequency, the resonant converters have better EMI performance than the PWM converter as shown in Figure 2.8. An experimentally tested topology selection procedure for EMI minimization in power supplies is presented in this paper [19].

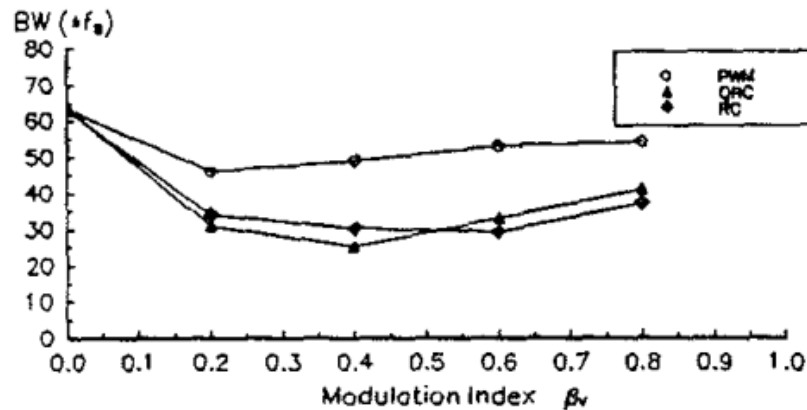


Figure 2.8: Bandwidth comparison among PWM, Quasi-resonant converter (QRC) and resonant converter (RC)

2.4 Review of Resonant Converter Topologies

In this section, the three main topologies of resonant converter are being reviewed. The discussion about these topologies about its primary architecture and characteristics specifically and provided with a view towards selecting the proposed converter for this work.

2.4.1 Series resonant converter (SRC)

Resonant inductor L and resonant capacitor C connect in series to form a resonant tank which is why it is called series resonant as shown in Figure 2.9. The series resonant tank functions like a current source. A capacitive filter C_o is required at output side to match the impedance. Resonant tank circuit and output load R_o form a voltage divider network. Because of this, the gain of the tank is limited to be less than one or equal to one [20]. When load or input voltage varies, changing the impedance of resonant tank will maintain the consistent voltage across the load. By varying the switching frequency according to the load, the impedance of resonant tank can be controlled; hence the output voltage is regulated. To achieve zero voltage switching, SRC must operate at above resonance frequencies.

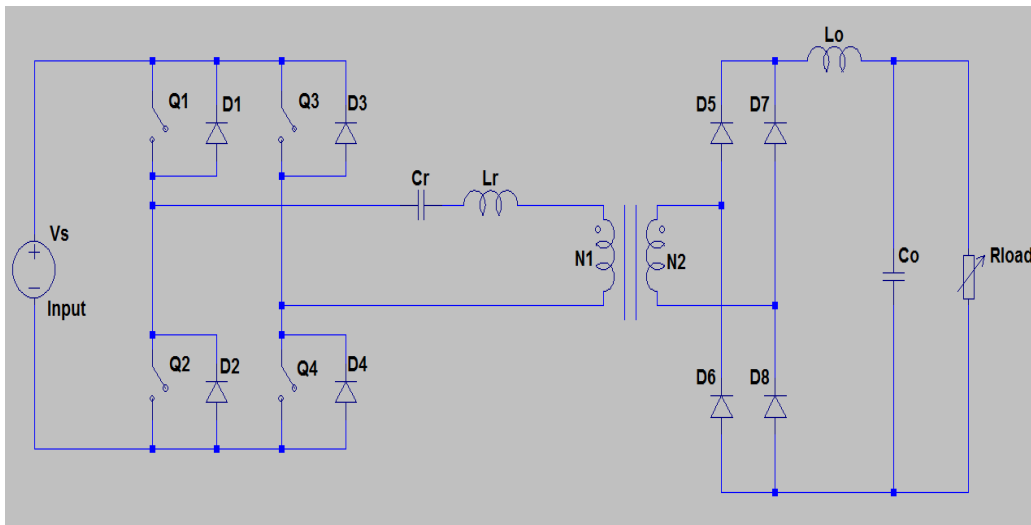


Figure 2.9: Example of series resonant converter

DC gain characteristic is given in Figure 2.10. It gives five curves with different Q values. From the curves or the formula given in figure, it can be observed that when output load increases Q values decreases, switching frequency is running much higher than the one with higher Q . For example, comparing the switching frequency difference between $Q=1$ and $Q=2$ with gain $M=0.6$, relative angular frequency is 1.6 for $Q=1$ while 1.2 for $Q=2$. Now if SRC in no-load condition, the converter could have trouble to control the output voltage by running frequency at infinitely high. Another drawback of series resonant converter is high ripple current need to be handled by output capacitor. It is not suitable for the application of low voltage high current converter where it requires very small ripples. To maintain these small ripples the required size output capacitance will be large. This may lead to use big number of capacitors and system components cost may increase. Although series resonant offers several advantages such as inherently providing high impedance against short circuit, two big disadvantages prevent it from using for low voltage high current applications [16].

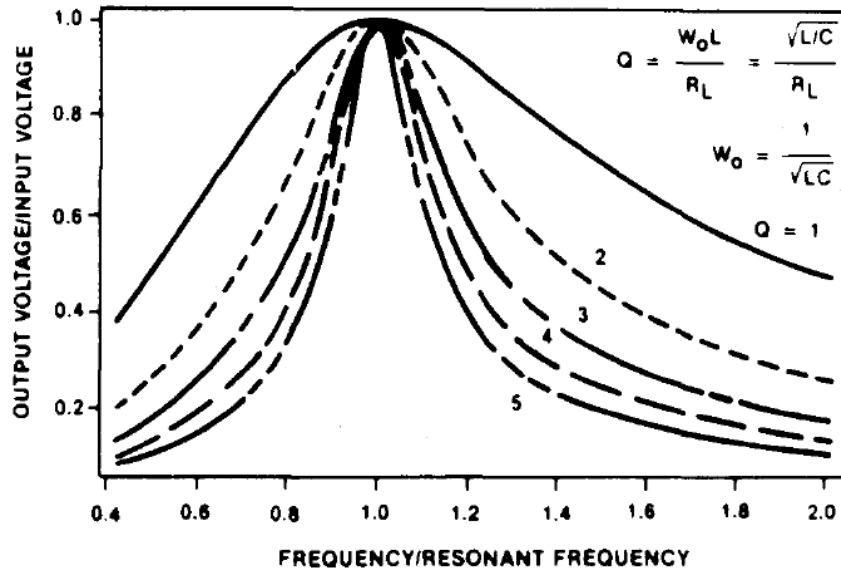


Figure 2.10: SRC converter gain curve for above resonance

Three main disadvantages of series resonant converter (SRC) as follow presented in [21]

- i. Switching frequency varies directly with the load which will cause poor cross regulation in multi-output power supplies
- ii. The ripple current in the filter capacitor is very high, potentially a challenge to control the output ripple voltage over the DC output.
- iii. SRC cannot operate at zero load.

2.4.2 Parallel resonant converter

Even though series resonant converter can achieve high efficiency for curtain applications, it is generally not a good candidate for low voltage high current converter application. Following figure shows the circuit diagram of parallel resonant converter. The resonant tank is formed by an inductor and a capacitor place across the input to the rectifier circuit as shown in Figure 2.11, hence this configuration is called parallel resonant converter.

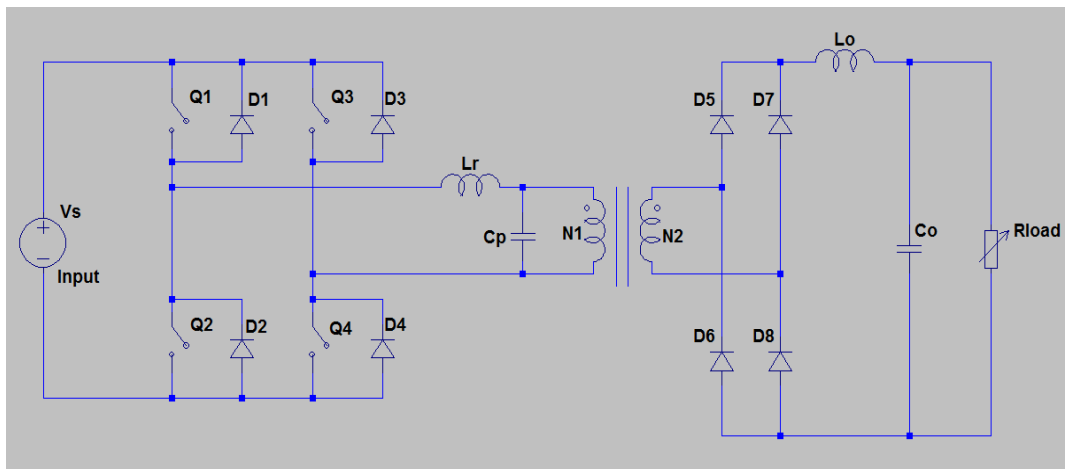


Figure 2.11: Example of parallel resonant converter

The resonant tank appears low impedance to the output circuit and is considered as a voltage source. An LC filter is placed in the output to march up the impedance. Compare to the current source type resonant converter, parallel resonant converter can achieve low output ripple by using relative low cost L-C filter. The DC characteristic gain curves for

parallel resonant converter are given in following Figure 2.12. As seen, in contrast to the series resonant converter, the converter can control the output voltage by running the frequency above resonance. The main disadvantage of the parallel resonant converter is high circulating current and it is relatively independent of load. It means that the conduction loss at light load is close to that at full load. The consequence of this characteristic is low efficiency of converter at light load. From the analysis above, it can be observed that parallel resonant converter is not a good candidate although it can provide low output ripple. High conduction loss at light load prevents the consideration.

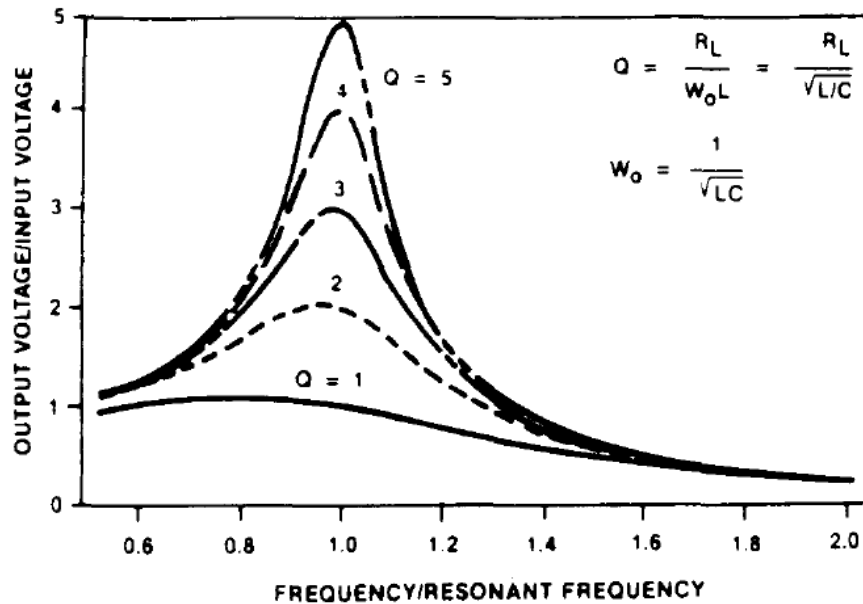


Figure 2.12: SRC converter gain curve for above resonance

2.4.3 Series-parallel resonant converter

Series-Parallel Resonant Converter (SPRC) takes the good characteristics of series and parallel resonant converter while eliminating their drawbacks, such as no-load regulation issue for series resonant converter and high circulating current at light load for parallel resonant converter [22]. The circuit diagram of series-parallel resonant converter is shown in Section 3.2. It consists of four sections which are high frequency inverter, resonant tank, output rectifier and output filter.

High frequency inverter provides bi-directional square waved signal that is fed into resonant tank. In resonant tank, there are three resonant components: L_s , C_s and C_p . The resonant tank of series-parallel resonant converter can be considered as the combination of resonant tanks of series and parallel resonant converter. By adding a series capacitor, C_s into parallel resonant tank, the circulating energy is smaller comparing with parallel resonant converter [23]. Notice in Figure 2.13, with the parallel capacitor C_p , series-parallel resonant converter can regulate the output voltage at no load condition. Parallel capacitor C_p provides low impedance that can be matched up by L-C type output filter by which low output ripple can be achieved easily.

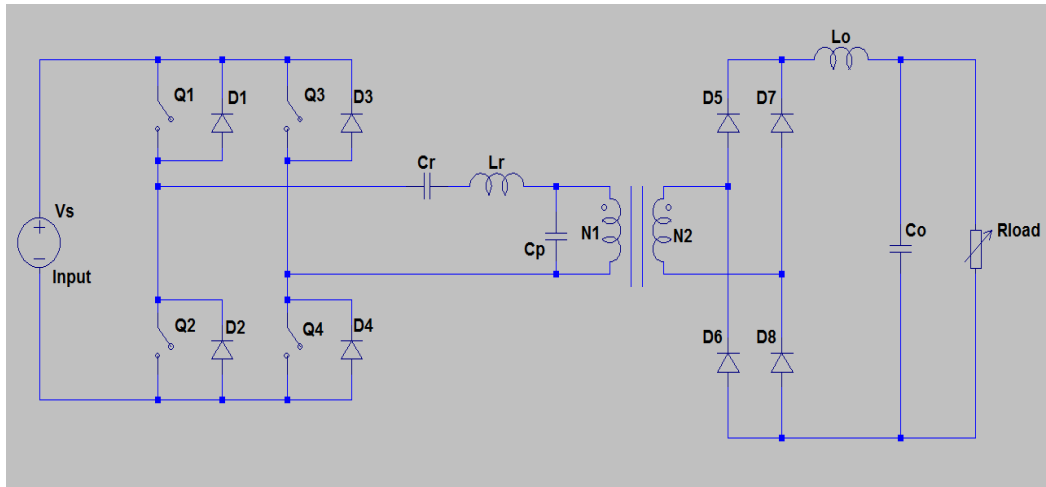


Figure 2.13: Example of series-parallel resonant converter

2.5 Resonant converter operation mode

Resonant converters can operate in following three modes:

(i) Below resonance mode

Switching frequency $f_s <$ Resonant frequency f_r is called below resonance mode. In this mode, the impedance seen by the inverter is capacitive. This means current i_s will be leading resonant tank input voltage V_s . With leading current, inverter effectively operates with zero current switching (ZCS). In continuous

current mode (CCM), power switches can only achieve ZCS during switches turn off at below resonance frequency, the turn-on is hard switching [24]. But with discontinuous current mode (DCM), soft-switching can be achieved for both turn-on and turn off [25]. This paper presented by Xing Tan has provide detailed analysis of optimized design of LCC resonant converter in DCM mode [26].

(ii) Resonance mode

Switching frequency $f_s =$ Resonant frequency f_r is called at resonance mode. In this mode, the impedance seen by inverter is resistive. Inductive and capacitive impedances are cancelling each other. Resonant tank input voltage V_s and current i_s both in phase, resonant converter gives maximum output in this mode. Maximum output can be realized when operating in this mode.

(iii) Above resonance mode

Switching frequency $f_s >$ Resonant frequency f_r is called above resonance mode. In this mode, the impedance seen by the inverter is inductive. This means current i_s will be lagging resonant tank input voltage V_s . With lagging current, inverter effectively operates with zero voltage switching (ZVS) as shown in Figure 2.14. During switch turn-on, the voltage across the drain-source V_{DS} is zero, hence the switching losses are eliminated

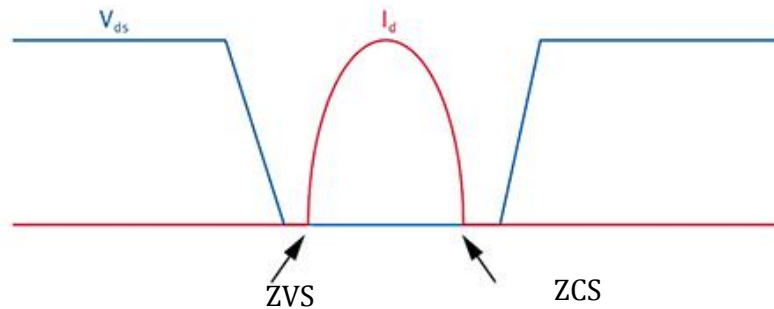


Figure 2.14: Soft switching voltage and current waveform

In all three converters the inverter circuit applies square wave of voltage to the resonant tank circuit and due to the resonant response, approximate sine waves of current are present in the resonant inductor L . The fact that the circuit is operating above resonance can be deduced from the fact that the current delivered to the resonant circuit is lagging the voltage applied to the resonant tank. No switching loss in above resonance operation because Q_1 is turned on during D_1 conduction interval where body diode carries current and the voltage across the Q_1 should be zero before it conducts forward current. Given in Figure 2.15, conduction sequence is $D_1/D_4 \rightarrow Q_1/Q_4 \rightarrow D_2/D_3 \rightarrow Q_2/Q_3$, assuming parasitic capacitances are negligible.

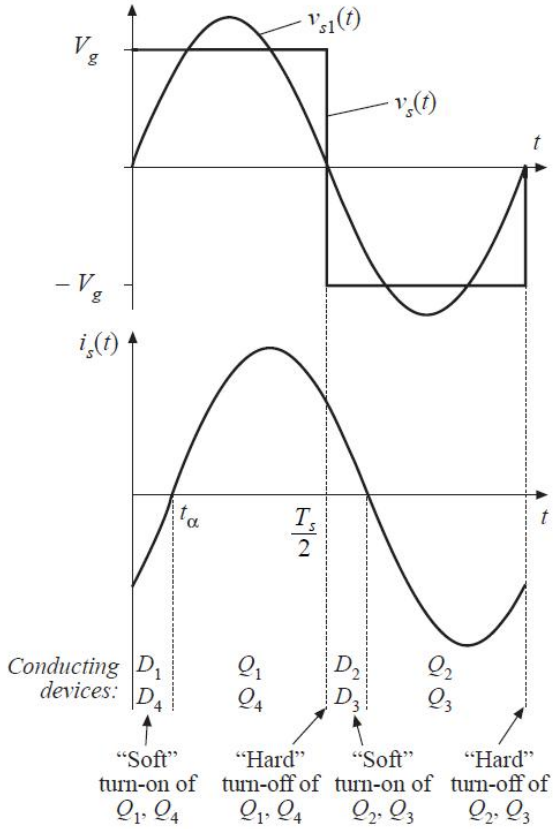


Figure 2.15: Example of voltage and current operating at above resonance

For the purpose of this work, only above resonance mode is considered because operating in this mode will help to avoid diode or MOSFET switching losses problem. Despite those advantages, MOSFET turning off switching losses should be taken into

consideration. In order to solve this concern, lossless snubber which can be a small capacitor should be placed directly across high side MOSFET which will be discharged by the load current thru inverse parasitic diode of high side MOSFET. To explain the above resonant mode, refer to the figure below as explained in. From the figure it appears that no turn-on switching losses because the body diode carries current and the voltage across MOSFET is zero before it conducts forward current. The inverse MOSFET current is caused by the complementary MOSFET turning off. For example, if the bottom switch turns off, the current that was in that switch is transiently maintained by the inductive action of the resonant inductor, which forces the current to flow through the high side switch in the inverse direction which is through its inverse parasitic diode.

Now compare the switching methodology to hard-switching as shown in Figure 2.16. Q1 turns on while D2 is conducting. Stored charge of D1 and related semiconductor output capacitance must be removed hence the spike is observed in the Q1 current which contributes to the switching loss.

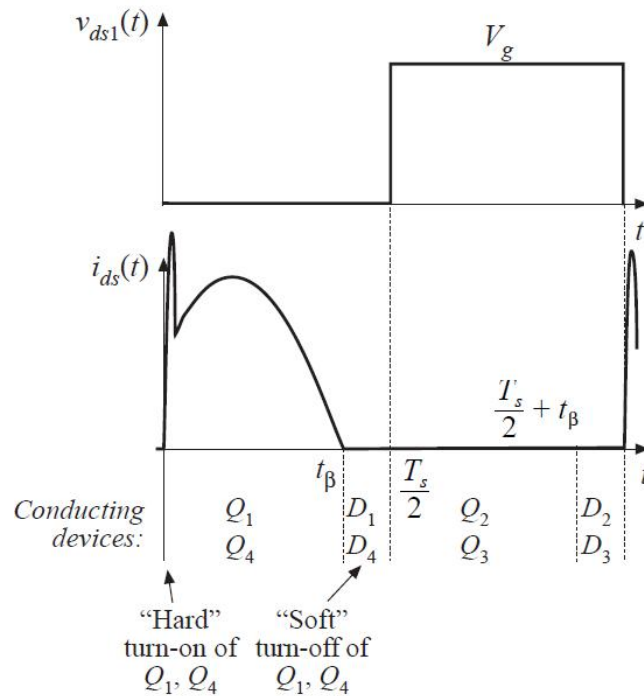


Figure 2.16: Possible spikes on waveform due to hard switching.

CHAPTER 3

METHODOLOGY

3.1 Introduction

In order to achieve the objectives of this project a non-isolated series-parallel resonant DC-DC converter with high step-up gain is proposed in this chapter. The structure of the proposed converter is described in section 3.2. The steady state operation of converter is described in section 3.3. Typical steady state waveforms of the converter including modes of operation and equivalent circuits are presented in this section. Next in section 3.4 ac analysis of the circuit in which ac equivalent circuit is derived is presented. In section 3.5 the dc gain equation of converter is derived. Then the dc gain of converter is plotted against frequency ratio for various values of quality factor and the graphs obtained are presented in the same section. Finally, a discussion is provided about converter gain analysis of series-parallel resonant converter.

3.2 The Proposed Non Isolated DC-DC Converter

Figure 3.1 shows the circuit diagram of the proposed non isolated DC-DC converter. It consists of a dc voltage source, full-bridge inverter, series-parallel resonant tank circuit, full bridge rectifier, LC filter and output load resistor. The front end of the proposed non-isolated resonant converter consists of a voltage fed full-bridge inverter followed by a series-parallel resonant tank. The resonant network is made up of series resonant capacitor, series resonant inductor and parallel resonant capacitor also known as LCC. The function of the inverter is to generate square wave pulsating ac voltage. This ac voltage is applied at the input terminals of the resonant tank circuit. The output terminals of the tank circuit are connected to a full-bridge rectifier. The tanks circuit offer frequency